

AD-A065 117

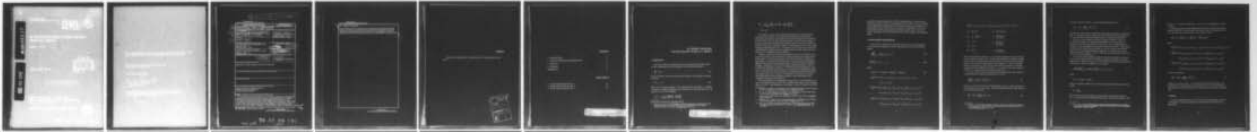
AIR FORCE GEOPHYSICS LAB HANSCOM AFB MASS
AN EFFICIENT BAROTROPIC VORTICITY EQUATION MODEL ON A SPHERE.(U)
NOV 78 S Y YEE
AFGL-TR-78-0273

F/G 4/2

UNCLASSIFIED

NL

| OF |
AD
A065117



END
DATE
FILMED
4 -79
DDC

DDC FILE COPY

ADA065117

9 Environmental research papers

Unclassified

SECURITY CLASSIFICATION OF THIS PAGE (When Data Entered)

REPORT DOCUMENTATION PAGE		READ INSTRUCTIONS BEFORE COMPLETING FORM
1. REPORT NUMBER 14 AFGL-TR-78-0273, AFGL-ERP-645	2. DOWNS ACCESSION NO.	3. RECIPIENT'S CATALOG NUMBER
4. TITLE (and Subtitle) 6 AN EFFICIENT BAROTROPIC VORTICITY EQUATION MODEL ON A SPHERE.	5. TYPE OF REPORT & PERIOD COVERED Scientific. Interim.	
7. AUTHOR(s) 10 Samuel Y. K. Yee	6. PERFORMING ORG. REPORT NUMBER ERP No. 645	
9. PERFORMING ORGANIZATION NAME AND ADDRESS Air Force Geophysics Laboratory (LYD) Hanscom AFB Massachusetts 01731	8. CONTRACT OR GRANT NUMBER(s)	
11. CONTROLLING OFFICE NAME AND ADDRESS Air Force Geophysics Laboratory (LYD) Hanscom AFB Massachusetts 01731	10. PROGRAM ELEMENT, PROJECT, TASK AREA & WORK UNIT NUMBERS 16 CDIOLP 23103200 17 G-2	13. NUMBER OF PAGES 22
14. MONITORING AGENCY NAME & ADDRESS (if different from Controlling Office) 12 22 p.	15. SECURITY CLASS. (of this report) Unclassified	
16. DISTRIBUTION STATEMENT (of this Report) Approved for public release; distribution unlimited.		
17. DISTRIBUTION STATEMENT (of the abstract entered in Block 20, if different from Report)		
18. SUPPLEMENTARY NOTES		
19. KEY WORDS (Continue on reverse side if necessary and identify by block number) Global numerical weather prediction Barotropic vorticity equation Filtered equation model		
20. ABSTRACT (Continue on reverse side if necessary and identify by block number) An efficient accurate algorithm for a barotropic model for a computational domain that encompasses the entire surface of the earth has been developed. While this simple model does not contain enough realistic features of the atmosphere to predict the synoptic-scale weather with accuracy, it does, however, simulate the planetary waves of the atmosphere with sufficient realism to enable us to conduct numerical experiments designed to study specific problems in numerical weather prediction. In this interim report, we shall give a		

DD FORM 1 JAN 73 1473 EDITION OF 1 NOV 65 IS OBSOLETE

Unclassified

SECURITY CLASSIFICATION OF THIS PAGE (When Data Entered)

79 02 26 134

409 578

YM

with page

Unclassified

SECURITY CLASSIFICATION OF THIS PAGE(When Data Entered)

20. Abstract (Continued)

brief discussion of the motivations for developing such a global barotropic model, describe in some detail the numerics for the solution of the model equations, and present some sample numerical time-integration results. Several remarks concerning the numerics of this algorithm are also included.

Unclassified

SECURITY CLASSIFICATION OF THIS PAGE(When Data Entered)

Preface

The author is indebted to Mr. Donald Aiken for his able assistance in this work.

ACCESSION for	
MFIS	White Section <input checked="" type="checkbox"/>
DDC	Buff Section <input type="checkbox"/>
UNANNOUNCED	
JUSTIFICATION	
BY	
DISTRIBUTION/AVAILABILITY COPIES	
Dist.	MAIL and SPECIAL
A	

Contents

1. INTRODUCTION	7
2. FINITE-DIFFERENCE APPROXIMATIONS	9
3. RESULTS	12
4. REMARKS	17
REFERENCES	21

Illustrations

1. Stream Function Field for $M_2 = 1$	14
2. Stream Function Field for $M_2 = 2$	15
3. Stream Function Field for $M_2 = 3$	16

An Efficient Barotropic Vorticity Equation Model on a Sphere

1. INTRODUCTION

The time evolution of planetary waves in the troposphere may be described, to a first approximation, by the barotropic vorticity equation (Rossby¹),

$$\frac{\partial \eta}{\partial t} = J(\eta, \psi) , \quad (1a)$$

where the absolute vorticity η and the stream function ψ must satisfy the physical constraint

$$\nabla^2 \psi = \eta - f . \quad (1b)$$

Here f is the Coriolis parameter. For a spherical earth with radius r , colatitude coordinate θ , longitude coordinate λ , and rotation rate Ω about the polar axis, the symbols in Eq. (1) are defined by

$$J(\eta, \psi) = \frac{1}{r^2 \sin \theta} \left[\frac{\partial \eta}{\partial \theta} \frac{\partial \psi}{\partial \lambda} - \frac{\partial \eta}{\partial \lambda} \frac{\partial \psi}{\partial \theta} \right] .$$

(Received for publication 9 November 1978)

1. Rossby, C. G. et al. (1939) Relation between variations in the intensity of the zonal circulation of the atmosphere and the displacements of the semi-permanent centers of action, J. Marine Res. 2:38-55.

$$\nabla^2 \psi = \frac{1}{r^2 \sin \theta} \left[\frac{\partial}{\partial \theta} \sin \theta \frac{\partial}{\partial \theta} + \frac{1}{\sin \theta} \frac{\partial^2}{\partial \lambda^2} \right] \psi ,$$

$$f = 2\Omega \cos \theta .$$

This model, by virtue of its realism and simplicity, has been extensively used in theoretical studies of the properties of atmospheric planetary waves. Among the large number of such studies reported in the meteorological literature, we may mention, for example, the classical work of Fjortoft² on the changes in the spectral distribution of atmospheric kinetic energy, and the work of Kuo³ and Lorenz⁴ on barotropic instability. Indeed, a model similar to this one was chosen, though with additional constraints, by Charney et al⁵ to be the first of a hierarchy of models used to conduct numerical weather prediction (NWP) experiments for a limited area covering most of North America.

However, a solution in spherical coordinates for this model, simple as it is, is not easy to obtain. Thus in the case of theoretical studies, an infinite β -plane approximation is commonly introduced to alleviate the geometric complexity of the problem. In the case of NWP applications, this model has been traditionally applied, using a polar stereographic projection, only to extra-tropical regions of the globe. Solving Eq. (1) for a limited region of the globe requires, however, artificial lateral boundary conditions. It is difficult and often impossible, to construct a set of boundary conditions which are consistent with the differential equations. But because the number of arithmetic computations needed for the numerical solution of Eq. (1b) on a sphere was prohibitive, the dilemma of imposing extraneous artificial lateral boundary conditions to the model equations was accepted in the past as a necessary evil.

With the development of computational mathematics, it is now possible to obtain an approximate solution to Eq. (1b) on a sphere with relatively little computing effort (cf. Yee⁶). It has thus become less taxing, in terms of computer resources,

2. Fjortoft, R. (1954) On the changes in the spectral distribution of kinetic energy for two-dimensional, non-divergent flow, Tellus 5:225-230.
3. Kuo, H.-L. (1949) Dynamic instability of two-dimensional non-divergent flow in a barotropic atmosphere, J. Meteor. 6:105-122.
4. Lorenz, E.N. (1972) Barotropic instability of Rossby wave motion, J. Atmos. Sci. 29:258-264.
5. Charney, J.G., Fjortoft, R., and von Neumann, J. (1950) Numerical integration of the barotropic vorticity equation, Tellus 2:237-254.
6. Yee, S.Y.K. (1976) An efficient method for a finite difference solution of the Poisson equation on the surface of a sphere, J. Computational Phys. 22: 215-228.

to conduct controlled experiments in NWP in a global setting. Among the problems which we plan to explore, using a global barotropic model, are the following: (1) the stability of barotropic flows on the surface of a sphere, (2) changes in the spectral distribution of kinetic energy in a barotropic atmosphere, (3) the effect of non-uniform spatial and temporal increments in a global model, and (4) the effect of assuming a "free-slip" boundary condition at the equator in a hemispheric model.

2. FINITE-DIFFERENCE APPROXIMATIONS

If we cover the surface of the earth with a grid formed by the intersections (i, j) of latitudes and longitudes, we may approximate Eq. (1) by the difference analogs

$$\left(\frac{\partial \eta}{\partial t}\right)_{i,j} \approx \frac{1}{r^2 m_i} J_{i,j}(\eta, \psi), \quad (2a)$$

$$\frac{1}{r^2} \nabla_{i,j}^2 \psi \approx \eta_{i,j} - f_{i,j}, \quad (2b)$$

where

$$J_{i,j}(x, y) = J_A(x, y) + J_B(x, y) + J_C(x, y) \quad (2c)$$

$$J_A(x, y) = (x_{i+1,j} - x_{i-1,j})(y_{i,j+1} - y_{i,j-1}) - (y_{i+1,j} - y_{i-1,j})(x_{i,j+1} - x_{i,j-1}),$$

$$J_B(x, y) = [y_{i,j+1}(x_{i+1,j+1} - x_{i-1,j+1}) - y_{i,j-1}(x_{i+1,j-1} - x_{i-1,j-1})] - [y_{i+1,j}(x_{i+1,j+1} - x_{i+1,j-1}) - y_{i-1,j}(x_{i-1,j+1} - x_{i-1,j-1})],$$

$$J_C(x, y) = [x_{i,j+1}(y_{i+1,j+1} - y_{i-1,j+1}) - x_{i,j-1}(y_{i+1,j-1} - y_{i-1,j-1})] - [x_{i+1,j}(y_{i+1,j+1} - y_{i+1,j-1}) - x_{i-1,j}(y_{i-1,j+1} - y_{i-1,j-1})].$$

$$\nabla_{i,j}^2 x \equiv a_i x_{i-1,j} + b_i x_{i+1,j} + c_i (x_{i,j-1} + x_{i,j+1}) - (a_i + b_i + 2c_i) x_{i,j} ,$$

$$x_{i,j} = x(\theta_i, \lambda_j) ,$$

$$m_i = 4 \Delta\theta \Delta\lambda \sin \theta ,$$

$$\theta_i = \left(i - \frac{1}{2} \right) \Delta\theta ,$$

$$a_i = \frac{\sin \theta_{i-1/2}}{\Delta\theta^2 \sin \theta_i} ,$$

$$\lambda_j = j \Delta\lambda ,$$

$$b_i = \frac{\sin \theta_{i+1/2}}{\Delta\theta^2 \sin \theta_i} ,$$

$$\Delta\theta = \pi/I ,$$

$$\Delta\lambda = 2\pi/J ,$$

$$c_i = \frac{1}{\Delta\lambda^2 \sin^2 \theta_i} ,$$

Here we have divided a latitude circle into J equal increments of $\Delta\lambda$ and a meridian into I equal increments of $\Delta\theta$. We have also excluded the coordinate singularities at the poles by constructing the grid in such a way that the poles are not grid points. This is done by placing the first grid-latitude at $\theta_1 = \Delta\theta/2$. The finite-difference Jacobian $J_{i,j}$ in Eq. (2) is due to Arakawa,⁷ except that it has been modified here for the spherical coordinates. A second order five-point centered-difference formula has been used for the Laplacian $\nabla_{i,j}^2$.

If we now discretize the time derivative in the left hand side of Eq. (2a) by a centered-difference "leap-frog" approximation, we have

$$\left(\frac{\partial \eta}{\partial t} \right)_{i,j}^n \simeq \left(\eta_{i,j}^{n+1} - \eta_{i,j}^{n-1} \right) / 2 \Delta t \quad (3)$$

where Δt is the size of the time increment and $\eta_{i,j}^n \equiv \eta(\theta_i, \lambda_j, n\Delta t)$ is the value of η at grid-point (i, j) and time-step n. With these approximations in space and time, Eq. (2a) now takes the form

$$\eta_{i,j}^{n+1} = \eta_{i,j}^{n-1} + \frac{2 \Delta t}{r^2 m_i} J_{i,j}^n (\eta, \psi) . \quad (4)$$

7. Arakawa, A. (1966) Computational design for long-term numerical integration of the equations of fluid motion: two-dimensional incompressible flow, 1, J. Computational Phys. 1:119-143.

For the very first time-step, we use forward-differencing in time,

$$\eta_{i,j}^1 = \eta_{i,j}^0 + \frac{\Delta t}{r^2 m_i} J_{i,j}^0(\eta, \psi) . \quad (5)$$

By and large, these are the difference formulae which we shall use to approximate Eq. (1). We shall, however, experiment with the flexible-increment approximation described below for possible improvements in computational efficiency.

One of the more troublesome numerical aspects in getting a solution for Eq. (2) is the problem of computational instability due to the convergence of meridians of the spherical coordinates at the poles. For a constant angular increment $\Delta\lambda$, the convergence of the meridians causes a decrease, on approaching the poles, of the linear spatial increment $\Delta s = \Delta\lambda r \sin \theta$ along a grid-latitude. Thus in order to maintain computational stability, we must use very small Δt values near the polar regions. Various schemes have been proposed in the literature to overcome this difficulty.

In a previous study in connection with the efficient finite-difference solution of Eq. (2b) on a sphere (Yee⁸), we adopted a computational scheme in which different sizes of angular increment are used at different latitudes to approximate the λ -derivatives. We write at latitude θ_i , for example,

$$\frac{1}{r \sin \theta_i} \left(\frac{\partial \psi}{\partial \lambda} \right)_{i,j} \simeq \frac{1}{r \sin \theta_i} \frac{1}{h_i 2\Delta\lambda} (\psi_{i,j+h_i} - \psi_{i,j-h_i}) , \quad (6)$$

where

$$\psi_{i,j+h_i} = \psi(i\Delta\theta, (j+h_i)\Delta\lambda) .$$

Here h_i is a positive integer which is less than J and is numerically closest to the number

$$h_i' = \frac{1}{\sin \theta_i} .$$

The restriction that h_i be integers is necessary here to insure that the points $(i, j+h_i)$ coincide with the computational grid points. With this formulation, since

8. Yee, S.Y.K. (1977) An Efficient, Accurate Numerical Method for the Solution of a Poisson Equation on a Sphere, AFGL-TR-77-0246, Air Force Geophysics Laboratory, Hanscom AFB.

$h_i \sin \theta_i \simeq 1$, the linear increment $\Delta s_i = \Delta \lambda r h_i \sin \theta_i$ is approximately constant for all θ_i .

This approach has met with considerable success for a stable rapid solution method for Eq. (2b). We shall extend this concept to the time-integration of Eq. (2a). The difference Jacobian in Eq. (2c) now takes the form

$$\mathbf{J}_{i,j}^*(x, y) \equiv (\mathbf{J}_A^*(x, y) + \mathbf{J}_B^*(x, y) + \mathbf{J}_C^*(x, y))/3 \quad (7)$$

where

$$\mathbf{J}_A^*(x, y) \equiv (x_{i+1,j} - x_{i-1,j})(y_{i,j+h_i} - y_{i,j-h_i}) - (y_{i+1,j} - y_{i-1,j})(x_{i,j+h_i} - x_{i,j-h_i}),$$

$$\mathbf{J}_B^*(x, y) \equiv [y_{i,j+h_i}(x_{i+1,j+h_i} - x_{i-1,j+h_i}) - y_{i,j-h_i}(x_{i+1,j-h_i} - x_{i-1,j-h_i})] - [y_{i+1,j}(x_{i+1,j+h_i} - x_{i+1,j-h_i}) - y_{i-1,j}(x_{i-1,j+h_i} - x_{i-1,j-h_i})],$$

$$\mathbf{J}_C^*(x, y) \equiv [x_{i,j+h_i}(y_{i+1,j+h_i} - y_{i-1,j+h_i}) - x_{i,j-h_i}(y_{i+1,j-h_i} - y_{i-1,j-h_i})] - [x_{i+1,j}(y_{i+1,j+h_i} - y_{i+1,j-h_i}) - x_{i-1,j}(y_{i-1,j+h_i} - y_{i-1,j-h_i})].$$

And Eq. (4) becomes

$$\eta_{i,j}^{n+1} = \eta_{i,j}^{n-1} + \frac{2\Delta t}{r^2 m_i^*} \mathbf{J}_{i,j}^{*n}(\eta, \psi), \quad (8)$$

where $m_i^* = 4 \Delta \theta \Delta \lambda h_i \sin \theta_i$. We reiterate here that with this scheme, time-integration is to be performed at every grid point (i, j) . Only in the difference approximations to the λ -derivatives do we invoke the idea of variable increments in λ .

3. RESULTS

We have coded the model Eq. (2) in Fortran for test calculations in a CDC 6600 computer. In actual computations, we introduced the non-dimensional parameters

$$\begin{aligned}
t^* &= t\Omega, \\
\psi^* &= \psi/(r^2\Omega), \\
\eta^* &= \eta/\Omega,
\end{aligned}$$

so that Eq. (2) can now be written as

$$\frac{\partial \eta^*}{\partial t^*} = \frac{1}{m_i} \mathbf{J}_{i,j}(\eta^*, \psi^*), \quad (9a)$$

$$\nabla_{i,j}^2 \psi^* = \eta^* - 2 \cos \theta_i. \quad (9b)$$

This simple scaling reduces the amount of computation somewhat in our time-integration procedure. Grid resolutions of $\Delta\theta = \Delta\lambda = 2\pi/36$ and $\Delta t^* = 2\pi/24$ ($\Delta t = 1$ hr) have been used for the sample results given in this section. For initial conditions we used variations of the now classic Rossby-Haurwitz waves given by Phillips,⁹

$$\psi^* = -w_3 \cos \theta + w_2 \cos \theta \sin^m \theta \cos m\lambda. \quad (10)$$

Here m is the zonal wave number and w_2, w_3 are constants in units of Ω . Note that ψ^* in Eq. (10) increases with θ and is antisymmetric about the equator. In most so-called global time-integrations, symmetry of the wind field about the equator is assumed; and time-integrations are then carried out only for a hemisphere or portions of a hemisphere. In our time-integrations, the following initial fields have been adopted:

$$\psi^* = \cos \theta \sum_{m=m_1}^{m_2} w_2(m) \sin^m \theta \cos m\lambda(1 - \alpha(m) - 0.1\beta(\theta)) - w_3 \cos \theta. \quad (11)$$

Here $\alpha(m), \beta(\theta)$ are random numbers which fall within the range (0, 1). Note that random phase-shafts are permitted in Eq. (11), and the ψ^* field is now no longer antisymmetric about the equator. For $m_2 = m_1$ and $\alpha(m) = \beta(\theta) = 0$, however, Eq. (11) reduces to Eq. (10), which gives us an unperturbed initial field.

We present here in Figures 1 through 3 the stream function fields for the cases $m_2 = 1, 2,$ and 3 respectively. In each of these cases, m_1 is set to equal 1.

9. Phillips, N.A. (1959) Numerical integration of the primitive equations on the hemisphere, Mon. Wea. Rev. 87:333-345.

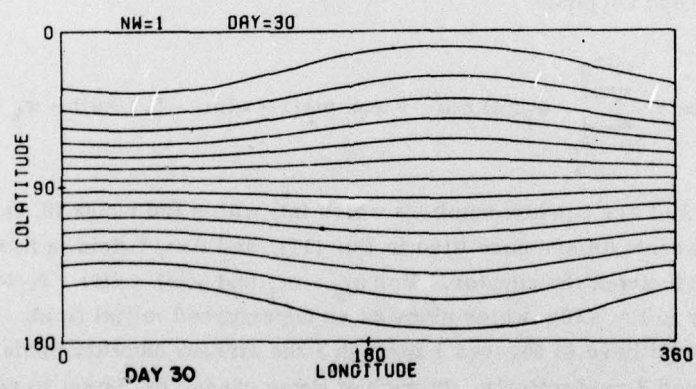
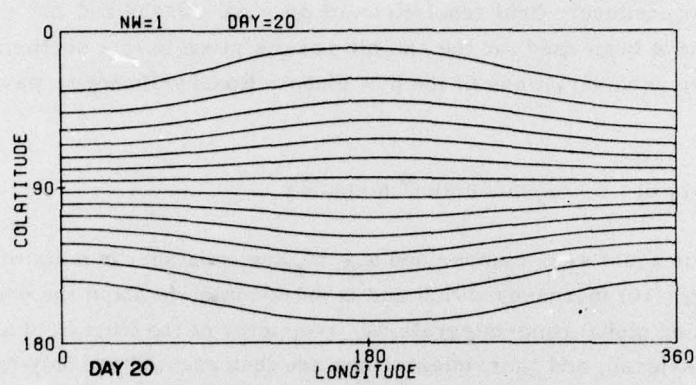
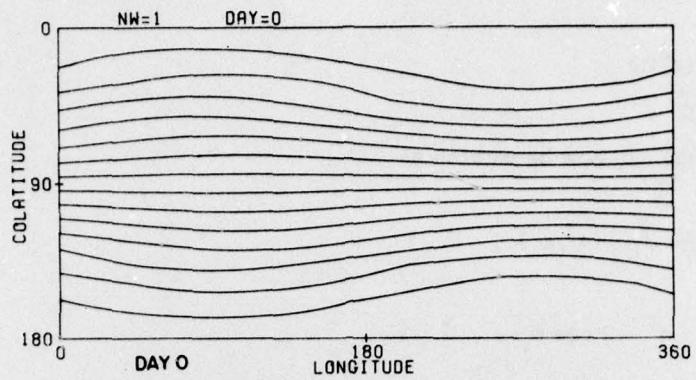


Figure 1. Stream Function Field for $M_2 = 1$

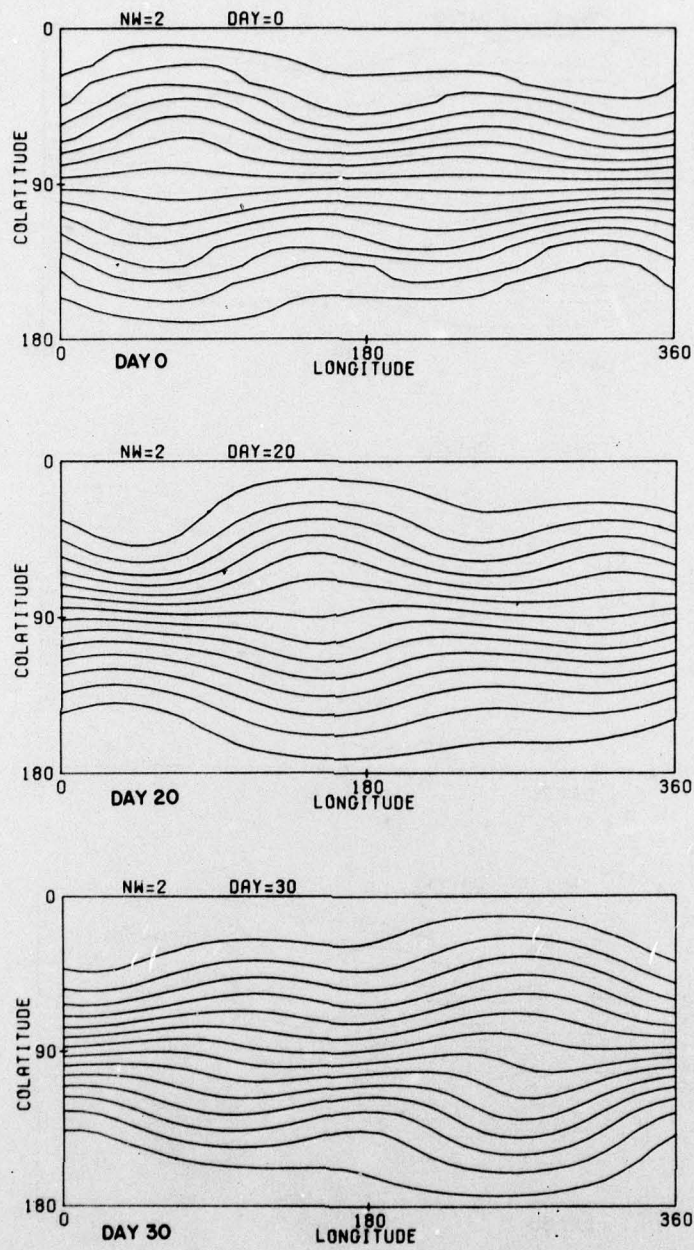


Figure 2. Stream Function Field for $M_2 = 2$

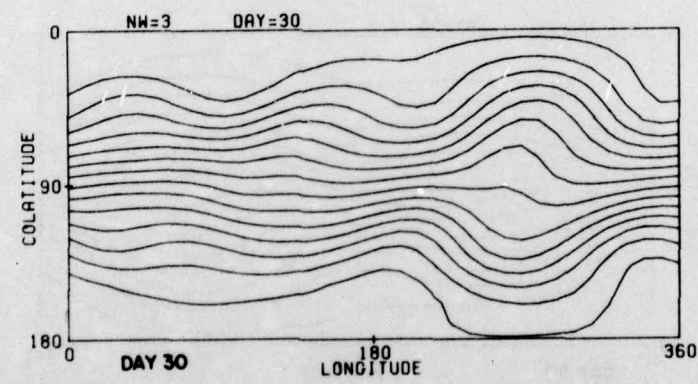
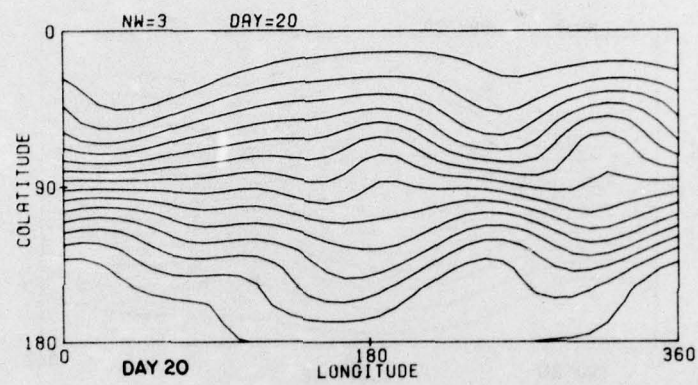
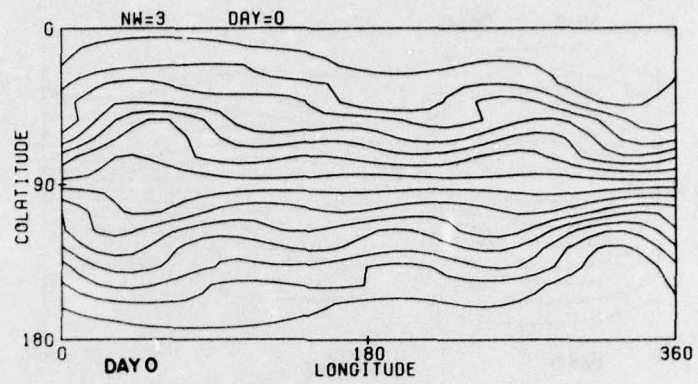


Figure 3. Stream Function Field for $M_2 = 3$

These figures are intended only to give a feeling of the time evolution of simple planetary waves in our model. We have examined more detailed model outputs and found that for the cases $m_1 = m_2$, $\alpha(m) = \beta(\theta) = 0$, the phase velocity of the waves in our model agrees well with that given by Phillips,⁹

$$\nu = \frac{m(m+3)w_3 - 2\Omega}{(m+1)(m+2)} \quad (12)$$

For example, for the case $m_1 = m_2 = 1$, $w_3 = 0.06\Omega$, the waves indeed retrograde at a constant angular velocity with a period close to 3.5 days. For the cases presented, time-integration was terminated arbitrarily after 30 model days. We have, however, integrated some cases with unperturbed initial fields ($m_2 < 3$) for up to 100 model days and detect no signs of numerical instability. Although not needed to maintain computational stability for the cases presented here, a 4th order linear filter designed by Shapiro¹⁰ has been applied at each time-step to the vorticity field. Present indications are that a Shapiro-type filter is needed to maintain numerical stability in long-term integrations for cases with $m_2 > 3$. In terms of central processor time, a typical integration of 2400 time steps takes roughly 260 sec in a CDC 6600. Thus both in terms of stability and efficiency, the algorithm reported here seems to be well suited for numerical experimentation.

4. REMARKS

(1) Many studies have been conducted on the numerical solution to barotropic models in spherical coordinates. These studies may be classified into two broad categories: those dealing with "filtered" vorticity equation models and those dealing with "primitive" shallow-water equation models. In the filtered equation models, fast moving gravity and sound waves are "filtered out" on physical grounds. Early numerical attempts (for example, Silberman,¹¹ Baer and Platzman¹²), to solve such model equations approximate the stream function with a finite sum of surface spherical harmonics, a natural choice for a basis function on a sphere.

10. Shapiro, R. (1978) Personal communications.

11. Silberman, I. (1954) Planetary waves in the atmosphere, *J. Meteor.* 11:27-34.

12. Baer, F., and Platzman, G.W. (1961) A procedure for numerical integration of the spectral vorticity equation, *J. Meteor.* 18:393-401.

This approach requires, however, a prohibitive amount of arithmetic computation. Thus only linearized flows or flows with two or three travelling waves were investigated.

The initial success of the barotropic vorticity equation model in operational NWP for a limited area (Cressman¹³) apparently spurred much interest in the 60's to formulate global finite-difference grids. The works of Gates and Riegel,¹⁴ Sadourny, Arakawa and Mintz,¹⁵ and Williamson¹⁶ are but a few examples of studies in this area.

With the realization that, in terms of NWP skills, the quasigeostrophic model has reached its theoretical plateau and that the next higher order approximation in filtered equation models involves mathematical difficulties, the tendency since the 60's has been to forego filtering out the fast waves and to return to the use of the "primitive" equation models. Beginning with Phillips,⁹ Kurihara,¹⁷ Grimmer and Shaw,¹⁸ Holloway, Spelman and Manabe,¹⁹ Williamson and Browning,²⁰ Kida,²¹ and Umscheid and Bannon²² among others have contributed to the numerical study of the barotropic primitive equation model on a sphere. Unlike the simple scheme described in Section 2, the majority of the work cited above resorted, however, to complicated computational design.

(2) With the advent of the fast Fourier transform, it has become more practical to perform time-integration of atmospheric models by the so-called pseudo-spectral

13. Cressman, G. P. (1958) Barotropic divergence and very long atmospheric waves, Mon. Wea. Rev. 86:293-297.
14. Gates, W. L., and Riegel, C. A. (1962) A study of numerical errors in the integration of barotropic flow on a spherical grid, J. Geophys. Res. 67:773-784.
15. Sadourny, R., Arakawa, A., and Mintz, Y. (1968) Integration of the non-divergent barotropic vorticity equation with an icosahedral-hexagonal grid for the sphere, Mon. Wea. Rev. 96:351-356.
16. Williamson, D. L. (1968) Integration of the barotropic vorticity equation on a spherical geodesic grid, Tellus 20:642-653.
17. Kurihara, Y. (1965) Numerical integration of the primitive equations on a spherical grid, Mon. Wea. Rev. 93:399-415.
18. Grimmer, M., and Shaw, D. B. (1967) Energy-preserving integrations of the primitive equation on the sphere, Quant. J. Roy. Met. Soc. 93:337-349.
19. Holloway, J. L., Spelman, M. J., and Manabe, S. (1973) Latitude-longitude grid suitable for numerical time integration of a global atmospheric model, Mon. Wea. Rev. 101:69-78.
20. Williamson, D. L., and Browning, G. L. (1973) Comparison of grids and difference approximations for numerical weather prediction over a sphere, J. Appl. Meteor. 12:264-274.
21. Kida, H. (1974) Tests of spherical grid systems for the primitive equations, J. Meteor. Soc. Japan 52:1-10.
22. Umscheid, L., and Bannon, P. R. (1977) A comparison of three global grids used in numerical weather prediction models, Mon. Wea. Rev. 105:618-635.

method discussed by Orszag.²³ Intense effort in recent years in this area of research has enabled the Canadian Atmospheric Environment Service to launch in 1976 the first spectral model into operational NWP (Daley et al²⁴). It is, however, not our purpose here to contrast the finite-difference method with the pseudo-spectral method.

(3) We may look at the differencing scheme given in Section 2 from two different points of view.

(a) A non-uniform angular increment $\Delta\lambda_i = h_i \Delta\lambda$ gives us a relatively constant linear increment Δs_i for all θ_i . Since h_i increases toward the poles, we have in effect, on approaching the poles, coarser and coarser resolutions in the λ -derivatives. The time-integration performed at every grid point is really nothing more than just a means by which we avoid altogether the problem of interpolation usually associated with a grid of mixed resolution.

(b) The use of a variable $\Delta\lambda_i$ for the λ -derivatives may also be interpreted as the use of a variable Δt_i in Eq. (8), for we may write Eq. (8) as

$$\eta_{i,j}^{n+1} = \eta_{i,j}^{n-1} + \frac{2\Delta t_i}{r^2 m_i} \mathbf{J}_{i,j}^{*n}(\eta, \psi),$$

where $\Delta t_i = \Delta t / h_i$. Since $h_i \approx 1/\sin \theta_i$, Δt_i decreases toward the poles. Thus the poleward increase of $\Delta\lambda_i$ in the evaluation of λ -derivatives is equivalent to keeping a uniform $\Delta\lambda$ but reducing the size of Δt_i on approaching the poles. This is somewhat similar to the method given by Grimmer and Shaw.¹⁸

(4) For our flexible differencing scheme, the truncation error in λ -derivatives increases toward the poles. This may turn out to be a problem for certain flow patterns as far as accuracy is concerned. This potential problem area deserves and will receive our closest attention.

23. Orszag, S.A. (1970) Transform method for calculation of vector coupled sums: application to the spectral form of the vorticity equation, J. Atmos. Sci. 27:890-895.

24. Daley, R., Girard, C., and Henderson, J. (1976) Short-term forecasting with a multi-level spectral primitive equation model, Part I - model formulation, Atmosphere 14:98-116.

References

1. Rossby, C. G. et al. (1939) Relation between variations in the intensity of the zonal circulation of the atmosphere and the displacements of the semi-permanent centers of action, J. Marine Res. 2:38-55.
2. Fjortoft, R. (1954) On the changes in the spectral distribution of kinetic energy for two-dimensional, non-divergent flow, Tellus 5:225-230.
3. Kuo, H. -L. (1949) Dynamic instability of two-dimensional non-divergent flow in a barotropic atmosphere, J. Meteor. 6:105-122.
4. Lorenz, E. N. (1972) Barotropic instability of Rossby wave motion, J. Atmos. Sci. 29:258-264.
5. Charney, J. G., Fjortoft, R., and von Neumann, J. (1950) Numerical integration of the barotropic vorticity equation, Tellus 2:237-254.
6. Yee, S. Y. K. (1976) An efficient method for a finite difference solution of the Poisson equation on the surface of a sphere, J. Computational Phys. 22: 215-228.
7. Arakawa, A. (1966) Computational design for long-term numerical integration of the equations of fluid motion: two-dimensional incompressible flow, 1, J. Computational Phys. 1:119-143.
8. Yee, S. Y. K. (1977) An Efficient, Accurate Numerical Method for the Solution of a Poisson Equation on a Sphere, AFGL-TR-77-0246, Air Force Geophysics Laboratory, Hanscom AFB.
9. Phillips, N. A. (1959) Numerical integration of the primitive equations on the hemisphere, Mon. Wea. Rev. 87:333-345.
10. Shapiro, R. (1978) Personal communications.
11. Silberman, I. (1954) Planetary waves in the atmosphere, J. Meteor. 11:27-34.
12. Baer, F., and Platzman, G. W. (1961) A procedure for numerical integration of the spectral vorticity equation, J. Meteor. 18:393-401.
13. Cressman, G. P. (1958) Barotropic divergence and very long atmospheric waves, Mon. Wea. Rev. 86:293-297.

14. Gates, W.L., and Riegel, C.A. (1962) A study of numerical errors in the integration of barotropic flow on a spherical grid, J. Geophys. Res. 67:773-784.
15. Sadourny, R., Arakawa, A., and Mintz, Y. (1968) Integration of the non-divergent barotropic vorticity equation with an icosahedral-hexagonal grid for the sphere, Mon. Wea. Rev. 96:351-356.
16. Williamson, D.L. (1968) Integration of the barotropic vorticity equation on a spherical geodesic grid, Tellus 20:642-653.
17. Kurihara, Y. (1965) Numerical integration of the primitive equations on a spherical grid, Mon. Wea. Rev. 93:399-415.
18. Grimmer, M., and Shaw, D.B. (1967) Energy-preserving integrations of the primitive equation on the sphere, Quant. J. Roy. Met. Soc. 93:337-349.
19. Holloway, J.L., Spelman, M.J., and Manabe, S. (1973) Latitude-longitude grid suitable for numerical time integration of a global atmospheric model, Mon. Wea. Rev. 101:69-78.
20. Williamson, D.L., and Browning, G.L. (1973) Comparison of grids and difference approximations for numerical weather prediction over a sphere, J. Appl. Meteor. 12:264-274.
21. Kida, H. (1974) Tests of spherical grid systems for the primitive equations, J. Meteor. Soc. Japan 52:1-10.
22. Umscheid, L., and Bannon, P.R. (1977) A comparison of three global grids used in numerical weather prediction models, Mon. Wea. Rev. 105:618-635.
23. Orszag, S.A. (1970) Transform method for calculation of vector coupled sums: application to the spectral form of the vorticity equation, J. Atmos. Sci. 27:890-895.
24. Daley, R., Girard, C., and Henderson, J. (1976) Short-term forecasting with a multi-level spectral primitive equation model, Part I - model formulation, Atmosphere 14:98-116.